Luo *et al. Biochar* (2026) 8:81
https://doi.org/10.1007/s42773-026-00591-2

Biochar

ORIGINAL RESEARCH Open Access

Biochar modulates temperature sensitivity of soil N_2O emissions: soil-specific mechanisms

Siyu Luo[1], Zhibo Li[1], Jing Hu[2] and Xiaolin Liao[1*]

Abstract

Biochar is increasingly promoted as a strategy for mitigating soil nitrous oxide (N_2O) emissions, yet its effect on the temperature sensitivity (Q_{10}) of N_2O emissions remains poorly understood. In this study, short-term incubation experiments were conducted using two contrasting soils (agricultural and forest soils) amended with two biochar types (wood- and rice husk-derived) at three application rates (0, 1%, and 3%) under three temperatures (10 °C, 20 °C, 30 °C). We investigated how biochar alters Q_{10} of N_2O emissions and explored the underlying mechanisms. Results showed that cumulative N_2O emissions increased with temperature in both soils, with higher Q_{10} values in forest soils (1.63–2.84) than in agricultural soils (1.13–1.63). Only high-rate wood biochar (WH) significantly changed Q_{10}, decreasing it in agricultural soils but increasing it in forest soils. In agricultural soils, WH strongly reduced NO_3^-–N availability and minimized its temperature response, intensifying substrate limitation and lowering Q_{10}. In forest soils, biochar accelerated the decline of NH_4^+–N and slowed the increase of NO_3^-–N with temperature, suggesting tighter coupling between nitrification and nitrate-consuming processes. Although WH and high rate rice-husk biochar showed the smallest NO_3^--temperature slopes, the unique properties of WH (e.g., low ash content, higher aromaticity, and larger pore size) may have promoted short-term NO_3^- retention, thereby strengthening temperature-coupled nitrification–denitrification turnover, which likely contributed to the higher Q_{10} observed under WH. Partial least squares path modeling (PLS-PM) confirmed that temperature exerted stronger total effects on N_2O emissions than biochar through changes in substrate availability, pH, and functional genes, while biochar acted as a secondary modulator. Overall, biochar regulated N_2O Q_{10} through soil-specific pathways, highlighting the need for soil-specific biochar application strategies under future climate change scenarios.

Highlights

- Biochar differently affected N_2O responses to warming in forest and farmland soils.
- Only high-rate wood biochar altered N_2O temperature sensitivity, lowering it in farmland but raising it in forest soils.
- Findings help guide tailored biochar strategies to control N_2O under climate change.

Keywords Q_{10}, Microbial functional genes, Nitrification, Denitrification, Path modeling

*Correspondence:
Xiaolin Liao
liaoxiaolin@njfu.edu.cn
Full list of author information is available at the end of the article

© The Author(s) 2026. **Open Access** This article is licensed under a Creative Commons Attribution 4.0 International License, which permits use, sharing, adaptation, distribution and reproduction in any medium or format, as long as you give appropriate credit to the original author(s) and the source, provide a link to the Creative Commons licence, and indicate if changes were made. The images or other third party material in this article are included in the article's Creative Commons licence, unless indicated otherwise in a credit line to the material. If material is not included in the article's Creative Commons licence and your intended use is not permitted by statutory regulation or exceeds the permitted use, you will need to obtain permission directly from the copyright holder. To view a copy of this licence, visit http://creativecommons.org/licenses/by/4.0/.

Springer

Graphical Abstract

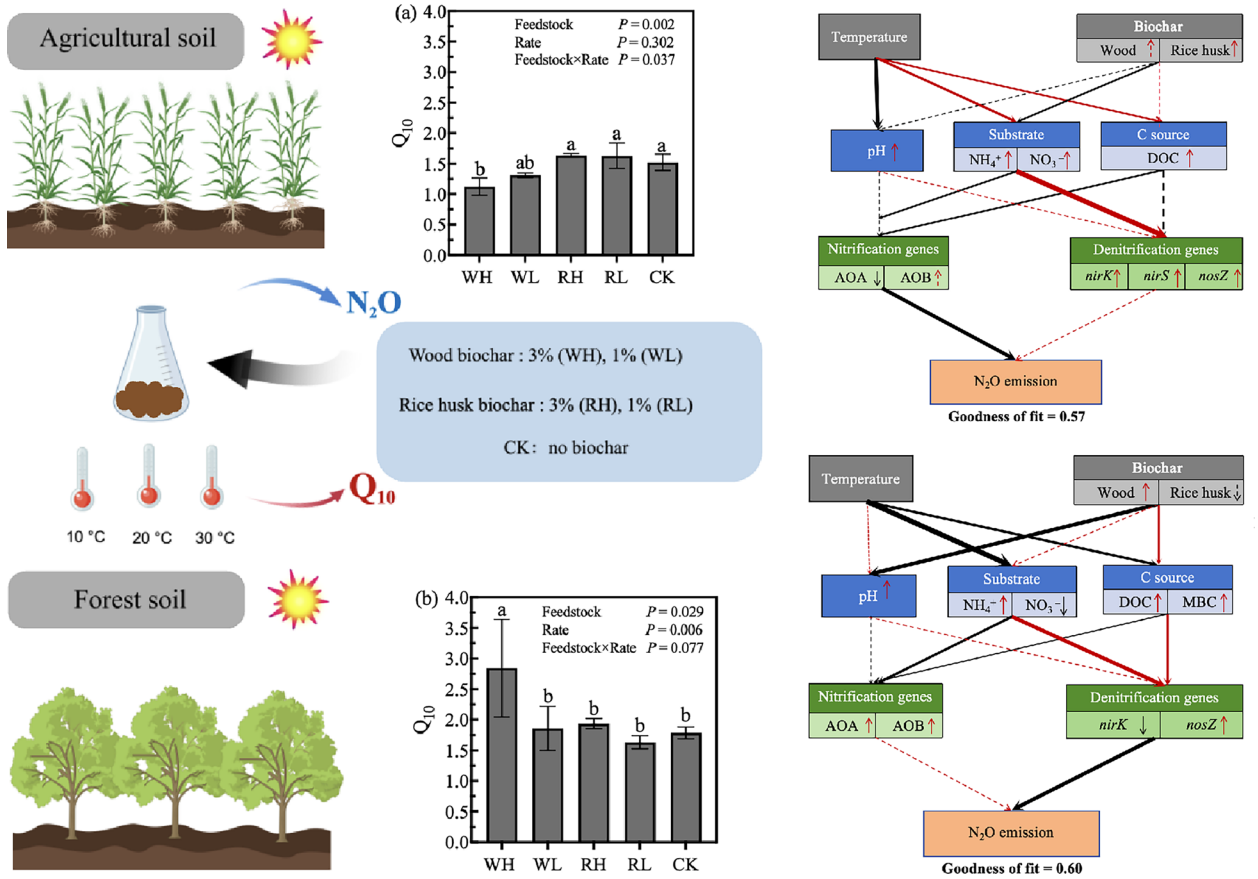

1 Introduction

Nitrous oxide (N_2O) is a potent and long-lived greenhouse gas, with a global warming potential 298 times that of carbon dioxide (CO_2) over a 100-year time frame (IPCC 2014). Its atmospheric concentration has steadily increased, largely due to anthropogenic nitrogen inputs into agricultural systems (Tian et al. 2020). Soils represent the primary natural source of N_2O, primarily through microbial processes such as nitrification and denitrification, which are sensitive to environmental and management factors including nitrogen inputs, soil moisture, and temperature (Butterbach-Bahl et al. 2013).

Biochar, a carbon-rich material produced by pyrolysis of biomass under limited oxygen, has gained considerable attention for its potential to mitigate soil greenhouse gas emissions while enhancing soil fertility (Xia et al. 2023). Numerous studies have demonstrated that biochar can reduce N_2O emissions by improving soil aeration, altering nitrogen availability, and modulating microbial activity (Cayuela et al. 2014; Liu et al. 2018). However, the effectiveness of biochar varies with soil type, feedstock properties, and application rate, and its interaction with environmental factors remains insufficiently understood (Nguyen et al. 2017; Zhou et al. 2025).

Temperature is one of the most important drivers of soil N_2O emissions, as it governs microbial activity and enzymatic kinetics involved in nitrogen cycling. Air temperature, which is closely correlated with soil temperature (Bond-Lamberty and Thomson 2010), is commonly used to represent thermal effects on microbial processes in Q_{10} studies (Song et al. 2018). The temperature sensitivity of biogeochemical processes is commonly described by the Q_{10} coefficient, which quantifies the rate change with a 10 ℃ increase in temperature (Davidson and Janssens 2006). Although Q_{10} values of soil CO_2 emissions have been extensively studied (Davidson and Janssens 2006; Meyer et al. 2018), those for N_2O are limited and less consistent, with reported values ranging widely (e.g., 1.44–72.2) (Sun et al. 2019) across ecosystems and soil types. Understanding the Q_{10} of N_2O

emissions is particularly relevant under climate warming, as it helps evaluate the strength and direction of feedbacks between temperature and microbial N transformation (Song et al. 2018).

The two major biological processes that contribute to soil N_2O production and consumption and consequently N_2O emissions respond differently to soil temperature. Ammonia-oxidizing archaea (AOA) and bacteria (AOB) exhibit distinct thermal optima and sensitivities, while denitrifying communities vary in their abundance and gene expression under warming (Avrahami and Conrad 2003; Tourna et al. 2008; Xing et al. 2021). For example, studies have shown that nosZ-type denitrifiers, which reduce N_2O to N_2, may be more responsive to warming than *nirK*-type denitrifiers (Cui et al. 2023; Dai et al. 2020). However, these microbial responses also depend on substrate availability (Cui et al. 2016; Song et al. 2018), which can be altered by biochar (Nguyen et al. 2017; Liu et al. 2018).

Recent studies have proposed that biochar–temperature interactions may jointly regulate N_2O emissions by modifying microbial metabolic efficiency and community composition under warming conditions (Rittl et al. 2021; Zhang et al. 2023a). Biochar can increase soil pH, reduce NO_3^- availability, and improve aeration, thereby shifting microbial nitrogen pathways and potentially modulating Q_{10} indirectly (Clough et al. 2013; Rogovska et al. 2011). Despite these insights, few studies have systematically examined how biochar affects the temperature sensitivity of soil N_2O emissions, particularly across different soil types or under varying application rates. Moreover, the mechanisms underlying such interactions remain poorly quantified.

Given the projected global warming and its influence on N_2O emissions, it is critical to evaluate how biochar affects the temperature sensitivity of soil N_2O fluxes, especially the link of biochar-induced shifts in microbial functional groups (e.g., AOA, AOB, *nirK*, *nosZ*) with changes in the Q_{10} of N_2O. In this study, we conducted controlled incubation experiments using two contrasting soils (agricultural and forest soils) and biochars derived from wood and rice husk applied at two rates. Our objectives were to (1) determine how biochar affects the Q_{10} of N_2O emissions across soil types, (2) assess the physcicochemical and microbial drivers underlying these effects; and (3) evaluate the relative importance of temperature and biochar using path modeling. This work aims to provide mechanistic insights into biochar–temperature–microbe interactions, contributing to a deeper understanding of how biochar can be used to mitigate N_2O emissions under climate warming scenarios, and providing guidance for tailoring biochar strategies to specific soil environments.

2 Materials and methods

2.1 Biochar and soil

The tested biochar samples included two types: rice husk biochar (R) and wood biochar (W). Wood biochar was produced from pine wood planks in a horizontal carbonization furnace (DLTH-1000) by heating at a rate of 7–13 ℃ min^{-1} to 500 ℃, followed by carbonization for 3 h and holding at that temperature for 2 h. Rice husk biochar was produced from rice husk feedstock in the same furnace following the same procedure as for wood biochar under pyrolysis conditions of 550 ℃ for 4–6 h. Both biochars were oven-dried at 80 ℃ for 48 h to a final moisture content of < 0.03% (w/w) before application.

Soil samples were collected from two sites, i.e., a wheat-soybean rotation system in Lishui District, Nanjing City, Jiangsu Province (31°46′14.08"N, 119°1′51.7"E), and a poplar (*Populus* spp.) plantation in Sihong County, Suqian City, Jiangsu Province (118°36′E, 33°32′N). These are hereafter referred to as agricultural and forest soil, respectively. The two soils are clay loam (Liao et al. 2025; Li et al. 2018). At each site, surface soil (0–20 cm depth) was collected, air-dried in the laboratory, and then sieved through a 2-mm mesh after removing stones and plant roots. Basic physicochemical properties of the soils and biochars were measured before incubation and are summarized in Table 1. Notably, the agriculture site had been abandoned and reclaimed only one year prior to sampling. This short reclamatoin history resulted in low fertility.

2.2 Incubation experiment

The two soils were subjected to the following treatments: a control without biochar addition (CK), and wood-derived biochar (W) and rice husk-derived biochar (R) applied at a high rate (3% w/w, H) and a low rate (1% w/w, L). These were designated as CK, WH, WL, RH, and RL, respectively. The incubation experiment was conducted in temperature-controlled incubators set at 10 ℃, 20 ℃, and 30 ℃ (air temperature, ± 0.5 ℃) with four replicates per treatment combination. Although soil temperature was not directly recorded, the set air temperature of the incubation chamber can be regarded as a proxy for soil temperature, as these two are generally well correlated under controlled conditions (Amato and Giménez 2024).

The incubation was conducted as follows. First, 100 g of soil sample was weighed into a 250 mL conical incubation flask. The moisture content was adjusted to 40% water-holding capacity (WHC), followed by a 3-day pre-incubation at each targeted temperature. Subsequently, 100 mg urea-N g^{-1} soil and biochar were mixed well into the soil, and the moisture content was readjusted to 70% WHC. Then, the formal incubation was implemented at the three designated temperatures for

7 days in agricultural soil and 10 days in forest soil. The choice of 7–10 days for incubation was based on our previous experiment (Liao et al. 2025) and literature reporting peak N_2O emissions within 5–10 days following nitrogen application (e.g., Zhang et al. 2019, 2023b; Wu et al. 2022). For example, Zhang et al. (2020a) used a 72-h incubation to measure N_2O emission rates and Q_{10} values in grassland soils, supporting the efficacy of short-term incubations for capturing microbial-driven N_2O dynamics.Throughout the incubation, flasks were sealed with perforated aluminum foil to minimize water loss through evaporation while maintaining aerobic conditions. Additionally, soil moisture was preserved by periodically replenishing deionized water to counteract evaporation losses.

2.3 Gas sampling

Gas sampling and N_2O analysis were conducted following the method established in our previously published study (Liao et al. 2025), with minor adaptations for soil-specific sampling intervals. Gas samples from agricultural soils were collected on days 1, 2, 4, and 7, whereas gas sampling for forest soil occurred on days 1, 2, 3, 5, 7, and 10. For each gas sampling event, the aluminum foil sealing the conical flasks was first removed to allow a 30-min equilibration period, ensuring the gas inside the flasks mixed well with the ambient atmosphere. The flasks were then resealed with airtight rubber septa and incubated for an additional hour before final sampling. Gas samples were collected using a three-way valve syringe, withdrawing 30 mL of headspace gas through the rubber septum. Samples were immediately transferred to 25 mL pre-evacuated vials (SVF-20, Nichiden-Rika, Kobe, Japan). Ambient air samples were collected prior to incubation initiation as baseline references ($t=0$). Gas concentrations were analyzed using a gas chromatograph (Agilent 7890B, USA) equipped with a ^{63}Ni electron capture detector. N_2O was quantified using the μECD detector with an argon-methane carrier gas mixture.

The gas flux was calculated as follows:

$$F = \rho \times \frac{V}{W} \times \frac{dc}{dt} \times \frac{273}{273 + T}$$

In this formula, F is the N_2O flux (ng N_2O-N g^{-1} h^{-1}), ρ is the N_2O density under standard conditions (μg N_2O–N m^{-3}), V is the volume of the headspace in the incubation flask (mL), W is the soil weight (g), T is the incubation temperature at sampling (℃), and dc/dt is the N_2O production rate during one hour.

With N_2O flux of each desired sampling date, the cumulative N_2O emissions over 7-day incubation period were calculated as

$$f = \sum_{i=1}^{n} (F_{i+1} + F_i)/2 \times (t_{i+1} - t_i) \times 24$$

In this formula, f is the N_2O cumulative emission (ng N_2O–N g^{-1}), F is the flux (ng N_2O–N g^{-1} h^{-1}), i is the sampling count, n is the total sampling events during the incubation, t is the sampling time, and t_{i+1}-t_i is the interval days between two samplings.

The temperature sensitivity parameter Q_{10} was calculated using the exponential equation method, with the calculation formula as follows (Ding et al. 2018):

$$F = \alpha \times e^{\beta T}$$

$$Q_{10} = e^{10\beta}$$

In this formula, F is the soil N_2O emission flux, α and β are the fitting parameters of the exponential equation, and T is the incubation temperature.

2.4 Destructive sampling and soil analysis

At the end of each incubation temperature treatment, destructive soil sampling was conducted, with each sample being divided into two portions. The first portion was stored at −4℃ in a refrigerator for subsequent analysis of nitrate nitrogen (NO_3^-–N), ammonium nitrogen (NH_4^+–N), and microbial biomass carbon (MBC). The second portion was air-dried in shaded conditions, then ground and sieved through 20-mesh sieves for determination of pH (soil: water = 1: 2.5).

Soil MBC was used as a proxy for microbial biomass activity (Joergensen and Mueller 1996) and was measured by the chloroform fumigation-K_2SO_4 extraction method. Microbial biomass nitrogen was not measured due to instrument constraints. Briefly, two fresh soil subsamples equivalent to 5 g dry soil weight were placed in 25 mL centrifuge tubes. One subsample was fumigated with alcohol-free chloroform for 24 h in the dark. Then, both the fumigated and non-fumigated subsamples were extracted with 0.05 M K_2SO_4 solution. The extracts were analyzed using a Shimadzu TOC-L CPH/CPN analyzer. The dissolved organic carbon (DOC) of the non-fumigated soil samples is soil DOC, while MBC was calculated by the difference between fumigated and non-fumigated extractable organic carbon contents and divided by a correction factor of 0.45 (Wu et al. 1990). For mineral nitrogen analysis, fresh soil samples were extracted with 1 M KCl solution, and the extract was analyzed for NH_4^+–N and NO_3^-–N concentrations using ultraviolet spectrometry (U-2900; HITACHI, Tokyo, Japan) following the indophenol blue methods (Zhang et al. 2023b).

Additionally, electrical conductivity (EC) and cation exchange capacity (CEC) were measured for the soils and biochars before incubation. EC for both soils and biochars was measured in a 1:5 (w/v) suspension using a conductivity meter (DDS-307, Rex, China). CEC was determined by compulsive exchange with 1 M NH_4OAc at pH 7.0 (Schollenberger and Simon 1945).

2.5 Abundance of N_2O-related functional genes

At the end of the incubation, functional genes related to N_2O emissions were measured in soils amended with low dose biochar (L) and control treatment (CK) due to resource limitations and field-realistic application rates. First, DNA extraction was performed using a PowerSoil DNA Isolation Kit, and DNA purity and quality were assessed via gel electrophoresis and a Nanodrop spectrophotometer, respectively. DNA was stored at −20 °C and diluted to 10 ng DNA μL^{-1} with sterile water for quantitative PCR (qPCR) analysis. The nitrification gene *amoA* was used to study the ammonia-oxidizing bacteria (AOB) and archaea (AOA), and the denitrification functional marker genes (*nirK*, *nirS*, and *nosZ*) were targeted. The two nosZ clades (I and II) were not analyzed separately because of low amplification efficiency of nosZII primers. The quantitative PCR (qPCR) was performed on a Step One Plus Real-Time PCR System (ABI, USA). Each qPCR reaction was performed in a 20 μL PCR mixture containing 10 μL SYBR@ Premix Ex Taq, 0.4 μL ROX reference dye (50×), 0.4 μL each primer, 2 μL template DNA, and 6.8 μL sterile water. The detailed information of primer and procedure was described in our previous study (Liao et al. 2021).

2.6 Statistical analysis

All data processing, statistical analyses, and graphical representations were performed using GraphPad Prism 10.0 software (GraphPad Software, California, USA). Each experimental treatment included four replicates, with data presented as mean ± standard error. A three-way analysis of variance (ANOVA) was used to test the effects of temperature, biochar feedstock, and biochar application rate on soil physcicochemical properties, and a two-way ANOVA was employed to examine differences in soil physicochemical properties and microbial indicators under the same incubation temperature, and Q_{10} values between different biochar feedstocks and application rates, followed by Tukey's honestly significant difference (HSD) post hoc test for multiple comparisons. Multivariate analysis was conducted using Pearson correlation coefficients to evaluate relationships and significance levels between various parameters, with statistical significance defined as $P < 0.05$.

The partial least squares path modeling (PLS-PM) analysis was performed to identify the pathways and main factors affecting N_2O emission using the R package "plspm" with 500 bootstraps. Model quality was assessed by the "goodness of fit" statistic. We first ran PLS-PM using only soil physicochemical properties and then incorporating the data of functional gene abundance.

3 Results

3.1 Effects of temperature and biochar on soil physicochemical properties

The effects of biochar on soil physicochemical properties (pH, DOC, NH_4^+–N, and NO_3^-–N) were interactively regulated by temperature, feedstock type, and application rate, with distinct responses observed between the two soil types (Table 2, Table S1).

Temperature effect: In agricultural soils, pH showed a significant drop when incubation temperature increased from 10 ℃ to 20 ℃ almost in all the treatments, while a similar drop in forest soils was only observed in CK (7.51, 7.15, and 7.29 at 10 ℃, 20 ℃, and 30 ℃, respectively). Conversely, soil DOC, NH_4^+–N, and NO_3^-–N in agricultural soils showed a significantly increase from 10 ℃ to 20 ℃ and 30 ℃. In forest soils, DOC was comparatively stable with rising temperature except showing an upward trend in WH and WL; NH_4^+–N exhibited a decreasing pattern with increasing temperature while NO_3^-–N significantly increased from 10 ℃ to 20 ℃ to 30 ℃.

Biochar effects: In agricultural soils, wood biochar notably increased soil pH under low-temperature conditions (10 ℃), particularly at high application rates (WH: 7.55 ± 0.03 vs. CK: 7.40 ± 0.03), while rice husk biochar showed no significant effect on soil pH (RH: 7.32 ± 0.02 and RL: 7.31 ± 0.02). In contrast, in forest soils, biochar application significantly decreased soil pH at 10 ℃ and 20 ℃, especially with the wood biochar and at high application rates. No significant effects of biochar on soil pH were detected at 30 ℃ in both soils.

Biochar generally showed no significant effects on dissolved organic carbon (DOC), except that WH significantly elevated soil DOC at 30 ℃ in agricultural soils (WH: 52.14 ± 2.59 vs.CK: 41.53 ± 3.71 mg kg^{-1}, $P < 0.05$) and at 10 ℃ in forest soils (36.11 ± 1.75 vs. 26.70 ± 0.97 mg kg^{-1}, $P < 0.05$).

Biochar feedstock, application rate, and their interaction significantly affected soil NH_4^+–N content only for agricultural soils at 10 ℃. Both wood and rice husk biochar decreased NH_4^+–N in agricultural soils, but only rice husk biochar showed significant reductions (RH: 0.13 ± 0.03, RL: 1.32 ± 0.28 vs. CK: 2.37 ± 0.30 mg kg^{-1}, $P < 0.05$).

Soil NO_3^-–N content generally responded negatively to biochar addition in both soils except at 10 ℃ in forest

soils. For example, in agricultural soils, WH significantly decreased NO_3^-–N content by 49.3%, 19.9%, and 76.4% at 10 ℃, 20 ℃, and 30 ℃, respectively. RH significantly decreased NO_3^-–N content by 48.3%, 35.8%, and 33.3% under 10 ℃, 20 ℃, and 30 ℃, respectively. In forest soils, WH significantly decreased NO_3^-–N content by 30.3% and 21.8% at 20 ℃ and 30 ℃, respectively, while RH significantly decreased NO_3^-–N content by 10.1% and 22.0% at 20 ℃ and 30 ℃, respectively.

3.2 Effects of biochar on soil N_2O emission

For agricultural soils, the temporal N_2O flux patterns from soils treated with RH and RL were similar to that from soils without biochar application (CK) (Fig. S1a–c). WH and WL treatments showed sharp N_2O peaks on day 1 (10 ℃), 3 (20 ℃), and 4 (30 ℃) after the urea application, respectively, and then the flux decreased to the baseline, while RH and RL peaked on day 2 post-urea application at 10 ℃. Significant increases in soil N_2O fluxes were observed only on day 1 after the urea application in WH and WL compared to CK at 10 ℃. In forest soils, N_2O fluxes from all treatments demonstrated similar temporal trends, with biochar generally reducing N_2O fluxes relative to the control (CK) (Fig. S1d–f). N_2O peaks occurred on day 7 (10 ℃), 5 (20 ℃), and 3 (30 ℃) after the urea application.

When upscaled to cumulative N_2O emissions, the biochar effects became more pronounced (Fig. 1). In agricultural soils, biochar feedstock showed significant effects on cumulative N_2O emissions only at 30 ℃ ($P<0.05$), while biochar rate significantly affected soil N_2O emissions at 20 ℃ and 30 ℃ (Fig. 1a). Specifically, at 10 ℃, WH decreased soil N_2O emissions by 10.9%, whereas WL, RH, and RL increased soil N_2O emissions by 16.1%, 16.5%, and 58.5%, respectively. At 20 ℃, WH, WL, RH, and RL enhanced cumulative N_2O emissions by 48.4%, 73.6%, 32.4%, and 44.3%, respectively. At 30 ℃, WH, WL, and RH decreased soil N_2O emissions by 40.0%, 10%, and 7.1%, respectively, with only WH showing significance (WH: 7.82 ± 0.25 ng N_2O–N g^{-1} vs CK: 13.03 ± 0.94 ng N_2O–N g^{-1}) ($P<0.05$); whereas RL significantly increased cumulative N_2O emissions by 16.9% (15.22 ± 0.95 ng N_2O–N g^{-1}) relative to CK.

In contrast, for forest soils, biochar feedstock type, application rate, and their interaction all exerted significant effects on cumulative N_2O emissions across all incubation temperatures ($P<0.05$, Fig. 1b). In general, biochar significantly decreased soil cumulative N_2O emissions. Specifically, WH reduced soil N_2O emissions by 99.5%, 80.1%, and 47.3%, respectively, at 10 ℃, 20 ℃, and 30 ℃; WL by 44.7%, 61.8%, and 38.7%, respectively; RH by 48.0%, 38.7%, and 22.7%, respectively; and RL by 58.3% and 8.1%, and 24.2%, respectively.

3.3 Effects of biochar on Q_{10} of soil N_2O emissions

Soil cumulative N_2O emissions from both agricultural and forest soils increased with the temperature across all treatments (Fig. 1). Specifically, for agricultural soils, all treatments showed relatively low emissions at 10 ℃ (3.53 ± 0.79 to 6.28 ± 1.14 ng N_2O–N g^{-1}), and increased at 20 ℃ (6.97 ± 1.97 to 12.10 ± 0.78 ng N_2O–N g^{-1}), and peaked at 30 ℃ (12.10 ± 1.47 to 15.22 ± 0.95 ng N_2O–N g^{-1}) (Fig. 1a). Forest soils followed a similar trend, with low emissions ranging from 0.12 ± 1.84 to 21.65 ± 2.75 ng N_2O–N g^{-1} at 10 ℃, increasing markedly at 20 ℃ (7.48 ± 2.64 to 37.50 ± 2.25 ng N_2O–N g^{-1}), and reaching even higher emissions at 30 ℃ (32.55 ± 1.07 to 61.81 ± 3.59 ng N_2O–N g^{-1}).

Accordingly, the temperature sensitivity (Q_{10}) of N_2O emissions in agricultural soils ranged from 1.01 to 1.90 among different biochar treatments. Both biochar feedstock type and its interaction with application rate significantly influenced Q_{10} values ($P<0.05$) (Fig. 2a). Notably, WH demonstrated the lowest Q_{10} (1.13 ± 0.08 vs CK: 1.52 ± 0.08). In comparison, forest soils exhibited consistently higher Q_{10} values ranging from 1.50 to 3.44 (Fig. 2b). Both biochar feedstock and application rate significantly influenced Q_{10} values ($P<0.05$). Interestingly, WH significantly increased Q_{10} (2.84 ± 0.46 vs CK: 1.79 ± 0.06), contrasting with its significant suppressing effect on Q_{10} in agricultural soils.

3.4 Effects of biochar and temperature on the abundance of soil N_2O-related functional genes

For agricultural soils, biochar application significantly influenced the abundances of AOB, *nirS*, *nirK*, and the (*nirS*+*nirK*)/*nosZ* ratio. Temperature exhibited significant effects on AOA, *nosZ*, and the (*nirS*+*nirK*)/*nosZ* ratio. The interaction between biochar and temperature significantly influenced the abundances of all five functional genes as well as the (*nirS*+*nirK*)/*nosZ* ratio. Specifically, AOA gene abundance increased significantly with rising temperature, especially between 10 ℃ and 20 ℃, while no further significant increase was observed between 20 ℃ and 30 ℃ (Fig. 3a). At 30 °C, WL showed significantly lower AOB gene abundance than both RL and CK (Fig. 3b, $P<0.01$). At 10 ℃, RL treatment exhibited significantly lower *nirS* abundance than WL (Fig. 3c, $P<0.05$), while at 30 ℃, WL and RL both significantly reduced *nirS* abundance compared to CK ($P<0.001$). WL also showed lower *nirS* abundance at 30 ℃ than at 20 ℃ and 10 ℃, in contrast to CK, which showed significantly higher *nirS* at 30 ℃. For *nirK*, RL treatment demonstrated a temperature-dependent increase (Fig. 3d), while WL maintained the lowest *nirK* abundance at 30 ℃ ($P<0.05$). The abundance of *nosZ* in soils treated with RL also increased with rising temperature, though

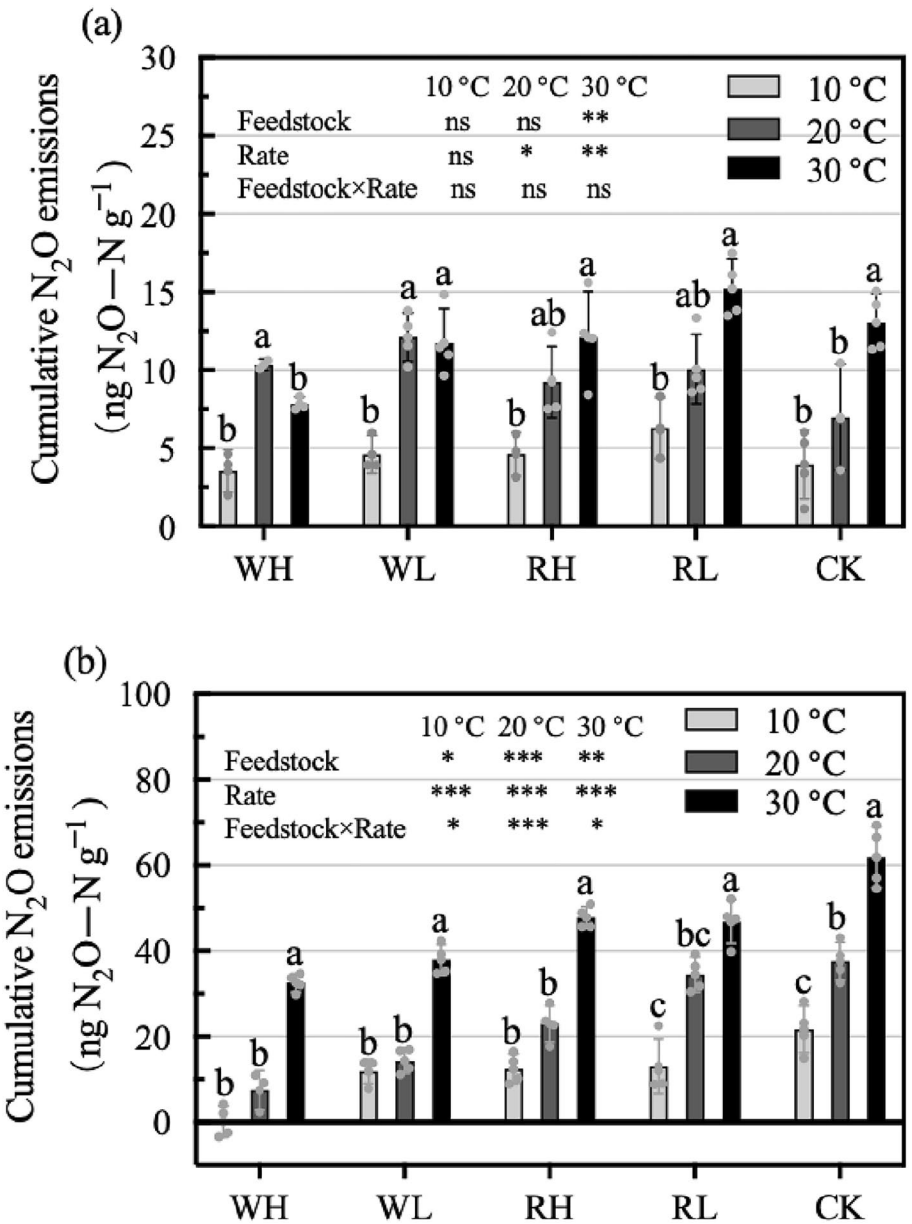

Fig. 1 N_2O cumulative emissions from agricultural soils (**a**) and forest soils (**b**) treated with different biochars during incubation. Different lowercase letters indicate statistically significant differences among different temperatures within the samebiochar treatment

biochar addition at 30 ℃ generally decreased *nosZ* gene abundance without statistical significance (Fig. 3e). At 20 ℃, WL treatment showed significantly higher (*nirS* + *nirK*)/*nosZ* ratio than RL (Fig. 3f, $P < 0.001$).

Forest soils exhibited microbial gene abundance approximately one order of magnitude higher than agricultural soils. Biochar application, temperature, and their interaction all significantly affected the abundances of AOA, AOB, *nirS*, *nirK*, *nosZ*, and the (*nirS* + *nirK*)/*nosZ* ratio (Fig. 3g–l). Specifically, AOA abundance increased significantly with temperatures, particularly at 30 ℃. Both WL and RL significantly increased AOA gene abundance at 30 ℃ compared to CK (Fig. 3g, $P < 0.05$). AOB abundance also increased significantly with temperature, with the highest levels at 20 ℃ ($P < 0.05$). At this temperature, WL showed lower AOB abundance than both RL and CK (Fig. 3h, $P < 0.05$). Compared to CK, WL significantly increased *nirS* gene abundance at 10 ℃, whereas RL significantly reduced *nirS* abundance at 20 ℃ ($P < 0.05$). Both WL and RL significantly suppressed *nirS*

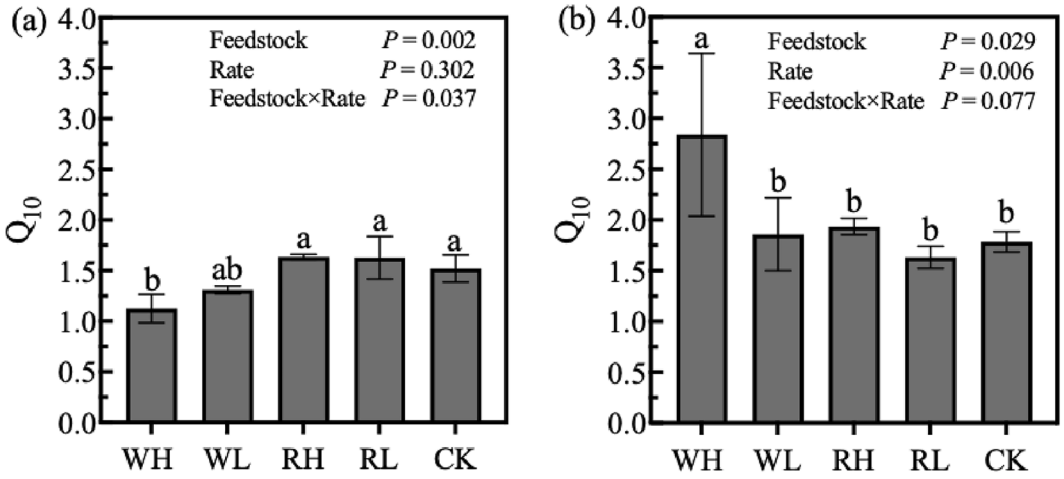

Fig. 2 Temperature sensitivity (Q10) of N_2O emissions from agricultural soils (**a**) and forest soils (**b**) treated with different biochars. Different lowercase letters indicate statistically significant differences among different biochar treatments

at 30 ℃ (Fig. 3i, $P<0.01$). Elevated temperature significantly increased *nirK* gene abundance, with the highest abundance at 30 ℃. WL treatment exhibited lower *nirK* abundance than RL at 20 ℃ (Fig. 3j, $P<0.01$). At 20 ℃, WL also demonstrated significantly lower *nosZ* gene abundance than both RL and CK (Fig. 3k, $P<0.01$). At 10 ℃, WL significantly increased the (*nirS*+*nirK*)/*nosZ* ratio than RL (Fig. 3l, $P<0.01$).

3.5 Drivers and regulatory pathways of soil N_2O emissions

In agricultural soils, correlation analysis (Fig. 4a) revealed that pH was significantly negatively correlated with DOC, inorganic nitrogen (NH_4^+–N, NO_3^-–N, SIN) and AOA abundance ($P<0.001$). Cumulative N_2O emissions were positively correlated with NH_4^+–N ($r=0.47$, $P<0.001$), NO_3^-–N ($r=0.63$, $P<0.001$), DOC ($r=0.48$, $P<0.001$) and AOA ($r=0.71$, $P<0.001$), but negatively correlated with pH ($r=-0.72$, $P<0.001$). Additionally, *nosZ* was positively correlated with *nirS* ($r=0.50$, $P<0.05$) and *nirK* ($r=0.74$, $P<0.001$).

In forest soils, pH was significantly negatively correlated with NH_4^+–N and MBC ($P<0.05$), but positively correlated with NO_3^-–N ($r=0.44$, $P<0.001$). N_2O emissions exhibited positive correlations with pH ($r=0.44$, $P<0.001$), NO_3^-–N ($r=0.85$, $P<0.001$), AOA ($r=0.63$, $P<0.01$), AOB ($r=0.62$, $P<0.01$), *nirK* ($r=0.75$, $P<0.001$), *nosZ* ($r=0.61$, $P<0.01$), and the (*nirS*+*nirK*)/*nosZ* ratio ($r=0.61$, $P<0.01$), but negative correlations with DOC ($r=-0.27$, $P<0.05$), NH_4^+–N and MBC ($r=-0.61$, $P<0.001$). AOA, *nirK*, *nosZ*, and (*nirS*+*nirK*)/*nosZ* were all significantly negatively correlated with NH_4^+–N ($P<0.01$) and significantly positively correlated with NO_3^-–N ($P<0.01$). AOA and AOB showed strong positive correlations with *nirK* and *nosZ* ($P<0.01$), and *nirK* was also significantly positively correlated with *nosZ* and the (*nirS*+*nirK*)/*nosZ* ratio ($P<0.01$).

To evaluate the relative contribution of abiotic and biotic factors to N_2O emissions, we first constructed PLS-PM using only physicochemical variables (Fig. S2), and then incorporated microbial functional gene groups in the models (Fig. 5). For agricultural soils, the PLS-PM further showed that temperature significantly reduced soil pH, and increased substrate availability (Fig. 5a, b). Biochar significantly reduced substrate availability but had no direct effect on N_2O emissions. Temperature, in contrast, had a significantly positive effect on soil N_2O emissions ($r=0.50$, $P<0.001$).

Interestingly, when both AOA and AOB were included as latent variables representing nitrification genes (Fig. 5a), nitrification showed a significantly negative correlation with N_2O emissions ($r=-0.66$, $P<0.001$). However, when AOB, which played a less prominent role and exhibited contrasting patterns with AOA, was removed, nitrification became significantly positively correlated with N_2O emissions (Fig. 5b), consistent with the multivariate correlation results (Fig. 4a). In contrast, denitrification genes showed no significant effect on N_2O emissions.

For forest soils, the PLS-PM (Fig. 5c, d) revealed that temperature exerted significantly negative effects on soil substrates and carbon sources, while biochar significantly decreased soil pH and increased soil carbon sources. Temperature had a stronger total effect than that of biochar, with the former significantly promoting N_2O emissions and the latter suppressing them.

Interestingly, when both biochars were included in the model, only denitrification genes showed a significantly negative correlation with N_2O emissions ($r=-0.68$,

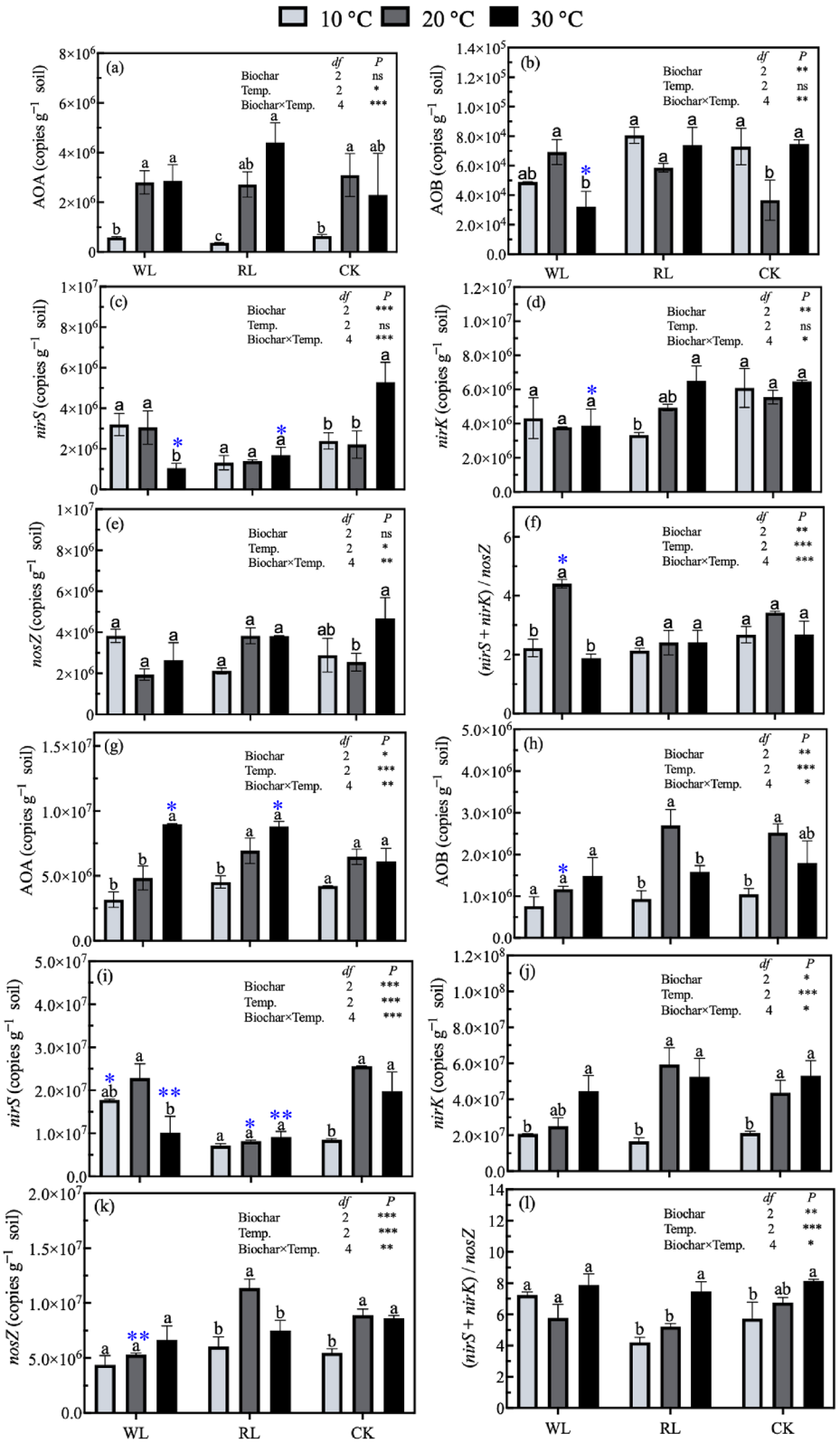

Fig. 3 Gene abundances of (**a**, **g**) AOA, (**b**, **h**) AOB, (**c**, **i**) *nirS*, (**d**, **j**) *nirK*, (**e**, **k**) *nosZ*, and (**f**, **l**) (*nirS* + *nirK*)/*nosZ* ratios in agricultural soils (**a**–**f**) and forest soils (**g**–**l**) treated with different biochars at varying temperatures. Different lowercase letters indicate significant differences betweem different temperatures unde same biochar treatment. Blue * on the top of the bars respresent significant difference from the control treatment (CK). *, **, and *** indicate significance at $P < 0.05$, $P < 0.01$, and $P < 0.001$, respectively

$P < 0.001$), while nitrification genes had no significant effect (Fig. 5c). When only rice husk biochar was retained in the model, both nitrification (positive) and denitrification (negative) genes significantly affected soil N_2O emissions (Fig. 5d).

4 Discussion

4.1 Temperature and biochar jointly influenced soil physcicochemical properties

Temperature and biochar jointly regulated soil physicochemical conditions, but their effects differed by soil type. In agricultural soils, pH consistently declined as temperature increased from 10 °C to 20 °C across treatments, whereas in forest soils, this decline was evident only in the control (CK). Such short-term acidification is commonly observed and attributed to enhanced microbial respiration and nitrification that release protons (H^+) into the soil solution (Yang et al. 2022).

Interestingly, our data showed no significant rise or even decrease in soil pH, creating an apparent contradiction with the cited literature on biochar's liming effect (Rogovska et al. 2011; Clough et al. 2013). This transient acidification was likely due to the strong buffering capacities of the near-neutral soils (Hailegnaw et al. 2019), the specific type and production temperature of the biochar we used having a lower pH or ash content (e.g., rice husk biochar) (Yao et al. 2025), and the release of weak organic acids from biochar surfaces or microbial production of acidic metabolites during early incubation (Lehmann et al. 2011). As temperature rose, these acids were progressively consumed or neutralized, and the pH in biochar treatments converged toward CK. Overall, the observed pH variations likely reflect a combination of temperature-enhanced microbial acid production and transient biochar–soil solution interactions, rather than a lasting acidification.

Dissolved organic carbon (DOC) showed distinct temperature responses between soils. Agricultural soils exhibited a marked DOC increase with incubation temperature, indicating enhanced solubilization of organic matter and enzymatic depolymerization under warming (Yu et al. 2025). In contrast, DOC in forest soils remained relatively stable, likely buffered by its higher organic carbon and stronger organo-mineral associations. Comparatively, biochar's effect on DOC was limited with only WH significantly elevating DOC at 30 ℃ in agricultural soils and at 10 ℃ in forest soils, likely due to the release of biochar-derived labile carbon release and temperature-dependent microbial decomposition and sorption processes.

Temperature also markedly altered soil inorganic N dynamics in contrasting ways between the two soils. In agricultural soils, both NH_4^+–N and NO_3^-–N increased from 10 °C to 30 °C, suggesting accelerated mineralization and nitrification under warming. In forest soil, NH_4^+–N declined while NO_3^-–N increased with temperature, indicating rapid conversion of ammonium to nitrate and a tighter coupling of ammonification and nitrification. These patterns indicate a more active and temperature-sensitive nitrogen cycle in forest soil, consistent with its higher SOC and nutrient contents.

Biochar effects on inorganic N were generally weaker than temperature but still exhibited clear patterns. Across both soils, biochar had negligible impact on NH_4^+–N, implying limited ammonium adsorption onto biochar surfaces or abiotic oxidation. In contrast, biochar consistently reduced NO_3^-–N, likely due to enhanced nitrate adsorption, denitrification, or microbial immobilization (Nguyen et al. 2017). The reduction was consistent across temperatures in agricultural soils, while in forest soils, it appeared mainly at 20 °C (WH and WL) and at 30 °C (all biochar treatments).

Together, these findings suggest that temperature drives the direction and magnitude of N transformations, while biochar modulates substrate availability, particularly nitrate, through short-term retention processes.

4.2 Temperature effects on N_2O emissions (Q_{10}): soil-specific sensitivity

The PLS-PM analysis highlighted the dominant role of temperature in regulating N_2O emissions (Fig. 5, Fig. S2). Cumulative N_2O emissions increased with temperature in both soils (Fig. 1). At 10 °C, low microbial activity suppressed nitrification and denitrification, resulting in minimal N_2O emissions across all treatments. This trend aligns with the reported optimal temperature ranges for nitrifiers (25–35 °C) and denitrifiers (30–65 °C) (Zhang et al. 2019).

Notably, the forest soil emitted more N_2O than the agricultural soil (Fig. 1), opposite to many reports (Tian et al. 2020). This difference likely arises because the forest soil in this study was collected from a poplar plantation rather than a natural forest and contained substantially higher total carbon, total nitrogen, soil organic carbon,

(See figure on next page.)

Fig. 4 Correlations between soil physicochemical properties, cumulative N_2O emissions, and microbial gene abundances in agricultural (**a**) and forest (**b**) soils. Red indicates positive correlations, blue indicates negative correlations, with color intensity representing the strength of correlation. *, **, and *** denote significance at $P < 0.05$, $P < 0.01$, and $P < 0.001$, respectively

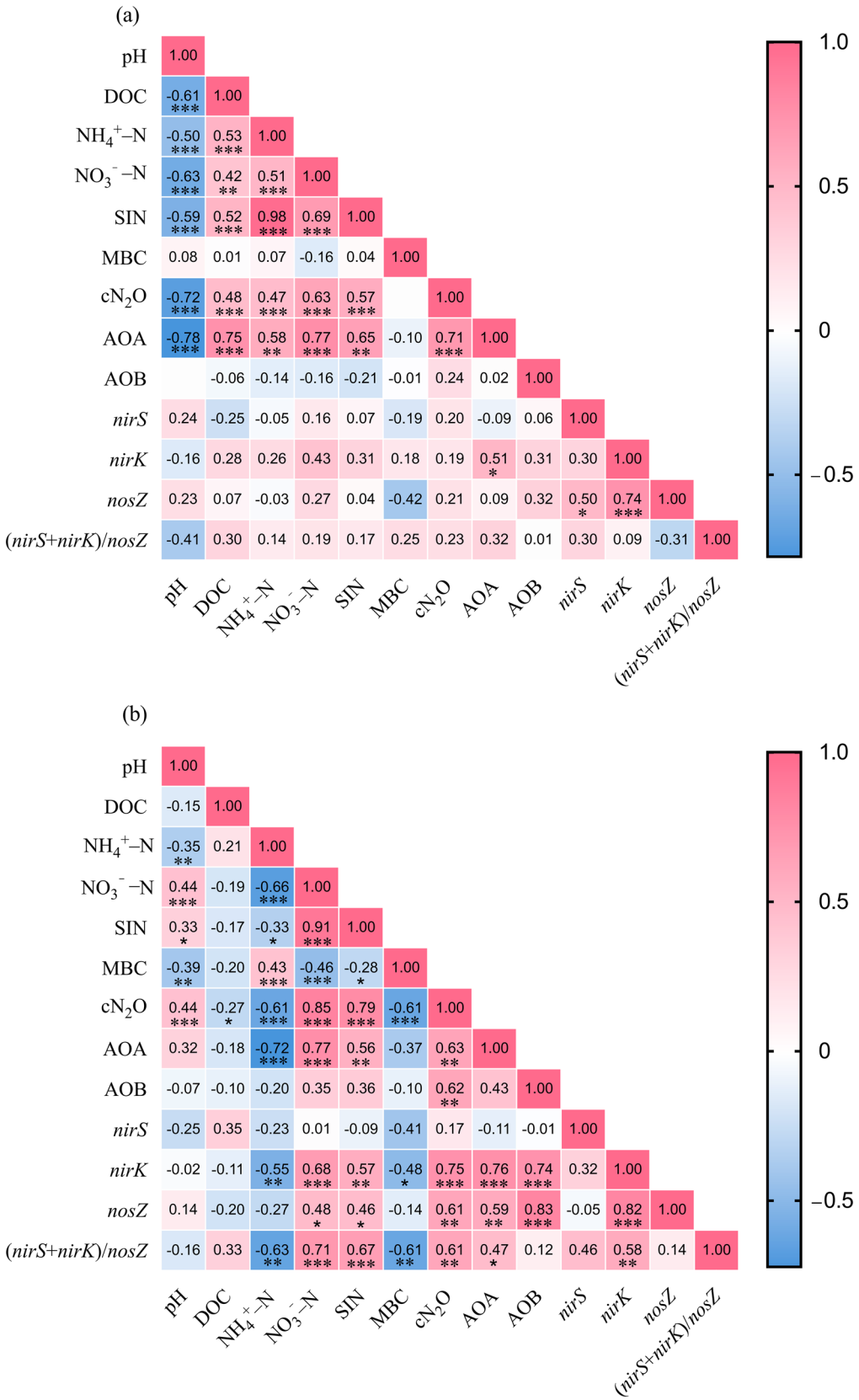

Fig. 4 (See legend on previous page.)

and mineral nitrogen contents than the recently abandoned-reclaimed agricultural soil (Table 1). These properties provided a larger substrate pool for microbial nitrification and denitrification, thereby sustaining higher N_2O emissions even during short-term incubation.

Temperature sensitivity of N_2O is often driven by soil fertility (Cui et al. 2016), texture (Cui et al. 2023), and organic carbon (Zhang et al. 2020b). In this study, forest soils showed higher Q_{10} values (1.63–2.84) than agricultural soils (1.13–1.63) (Fig. 2). This difference was primarily driven by inorganic nitrogen, with soil organic carbon (SOC) playing a synergistic supporting role. Inorganic nitrogen directly fuels nitrification/denitrification and thus sets the ceiling for temperature responsiveness. Specifically, in forest soils, abundant mineral nitrogen and higher SOC amplified warming responses and yielded higher Q_{10}.

Functional gene data further align with these interpretations. In agriculture soils, AOA exhibited an evident increasing trend with temperature (Fig. 3a), suggesting that AOA-driven nitrification may regulate the temperature sensitivity of N_2O. In forest soils, all five functional genes (AOA, AOB, *nirS*, *nirK*, and *nosZ*) responded significantly to temperature (Fig. 3g–l), implying co-regulation of nitrification and denitrification. The PLS-PM (Fig. 5, Fig. S2) further indicated temperature as the primary driver of N_2O and nitrification (AOA-mediated) dominated N_2O production in agricultural soils, while both nitrification and denitrification jointly contributed in forest soils. These distinct gene-level responses also help explain the higher Q_{10} in forest soils, where both N_2O production and reduction processes were actively temperature-sensitive.

4.3 Soil-specific effects of biochar on N_2O emissions

While temperature was the primary driver, biochar modulated N_2O fluxes through soil-specific pathways. It has been widely reported that biochar can reduce N_2O emissions (Cayuela et al. 2014, 2015; Liu et al. 2018). In this study, biochar's mitigation effect was observed in forest soils but was not consistent in agricultural soils (Fig. 1), emphasizing the dependence of biochar–N_2O interaction on soil types, biochar feedstock, pyrolysis conditions, and application rates (Cayuela et al. 2014, 2015; Liu et al. 2018).

In agricultural soils, biochar significantly lowered NO_3^-–N while leaving NH_4^+–N unchanged across temperatures, suggesting that changes in N_2O was not directly driven by enhanced nitrification but rather reflected indirect physicochemical effects (e.g., pH, DOC, micro-environment) that influenced nitrifier performance and potentially promoted denitrification. At 10 ℃ and 20 ℃, abundance of the five functional genes did not differ significantly among treatments, consistent with negligible effects of biochar on N_2O emissions. At 30 ℃, WL showed significantly lower abundance of AOB, *nirS*, and *nirK*, coincident with reduced N_2O in WL and WH. However, qPCR data failed to explain the significantly higher N_2O emissions in RL treatment at 30 ℃. These results suggest that biochar-induced changes in microbial functional groups were temperature-dependent and insufficient to fully account for the observed emission patterns. Correlation analysis across all treatments showed that N_2O emissions were positively related to DOC, NH_4^+–N, NO_3^-–N, and AOA abundance (Fig. 4a), indicating that substrate availability and temperature-driven nitrification dominated N_2O production, while biochar played an indirect, modifying role.

In forest soils, biochar, especially wood biochar, consistently reduced N_2O emissions across temperatures (Fig. 1b). This mitigation effect contrasts with the commonly reported liming effect (Clough et al. 2013; Rogovska et al. 2011), as pH decreased at 10 °C and 20 °C in biochar treatments. The reduction in NO_3^-–N under biochar treatments provides a plausible explaination for the suppressed N_2O fluxes. Lower nitrate availability likely constrained denitrification substrates, reducing N_2O formation (Mukherjee and Zimmerman 2013). qPCR shifts (e.g., WL/RL affecting AOA, *nirS*, *nosZ* at specific temperatures) did not align coherently with the uniform emission decreases, suggesting that short-term flux changes were not tightly coupled to gene abundance.

(See figure on next page.)

Fig. 5 Structure equation model (SEM) describing the effects of biotic factors on N_2O emission from agriculture soil with (**a**) and without (**b**) the indicator of AOB, and forest soil with (**c**) and without (**d**) wood biochar. The width of arrows is proportional to the strength of path coefficients. The red and black lines indicate positive and negative relationships, respectively. The continuous and dashed arrows in the boxes represent significant and insignificant relationships, respectively. Numbers adjacent to those arrows denote standardized path coefficients with significance. R^2 denotes the proportion of variance explained. The model includes the following variables: temperature, biochar, pH, substrate (NH_4^+ and NO_3^-), C source (DOC and MBC), nitrification genes, denitrification genes, N_2O emission, with "↑" and "↓" respectively indicating a positive correlation and a negative correlation between the latent variables in the rectangular boxes and the observed variables. The dashed arrows indicate insignificance. *, **, and *** indicate significance at $P < 0.05$, $P < 0.01$, and $P < 0.001$, respectively. The goodness of fit was used to assess the model

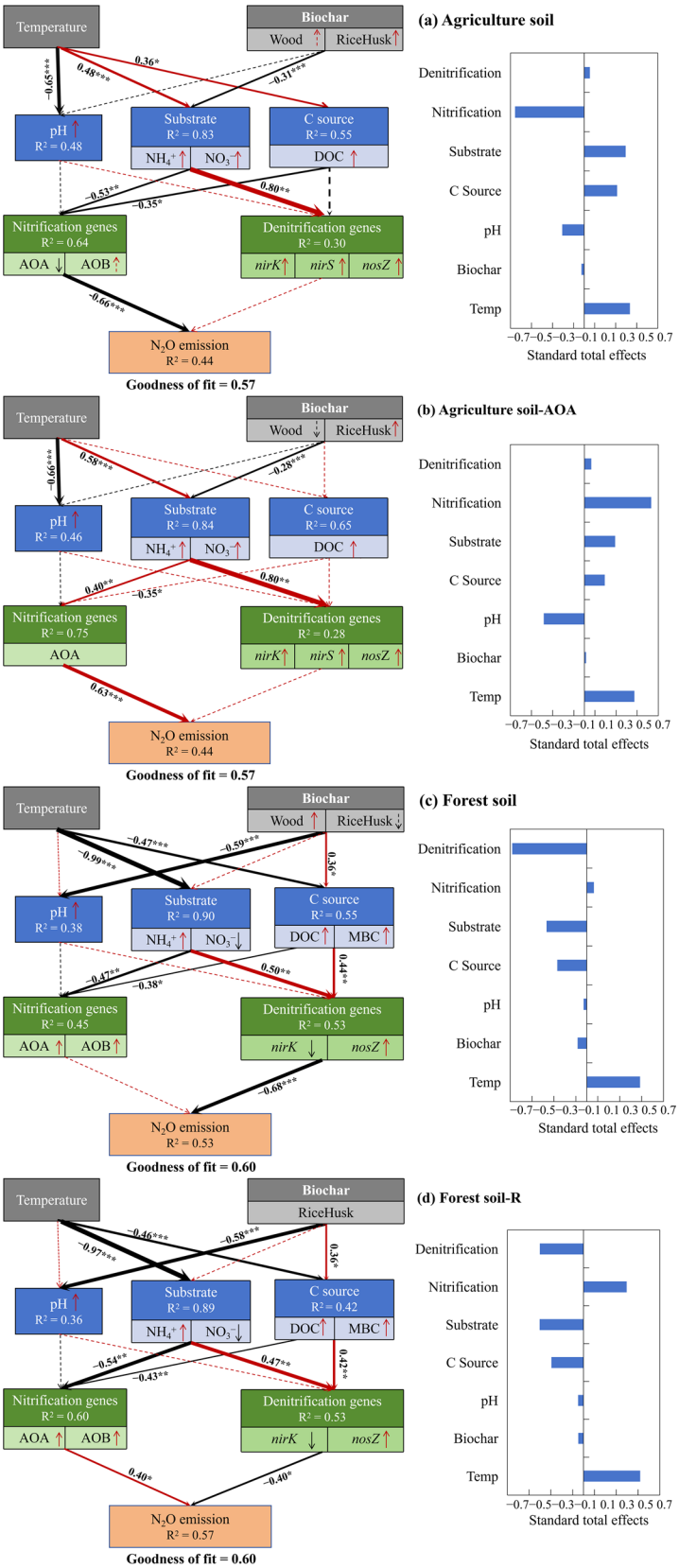

Fig. 5 (See legend on previous page.)

4.4 Biochar's modulation of the temperature sensitivity (Q_{10}) of soil N_2O emissions

Beyond regulating absolute N_2O emissions, biochar also influences their temperature sensitivity (Q_{10}) (Qi et al. 2020). Prior studies on biochar's effect on Q_{10} of N_2O are scarce and inconsistent: some reported no influence (Criscuoli et al. 2019), while others observed either increase (Deng et al. 2019) or short-term suppression (Criscuoli et al. 2024). In this study, only high-rate wood biochar (WH) significantly affected Q_{10} of N_2O emissions, decreasing it in agricultural soils but increasing it in forest soils (Fig. 2). This opposing response indicates that biochar effects on Q_{10} of N_2O are both dose- and soil-specific.

4.5 Agricultural soil: WH lowered Q_{10} by intensifing substrate limitation

The substrate-driven microbial response framework helps interpret these patterns (Song et al. 2018). Under limited substrate conditions, microbial growth and associated N_2O production become less responsive to temperature increases, resulting in a lower Q_{10} (Blagodatskaya et al. 2014; Zhang et al. 2020b; Velthuis and Veraart 2022).

In agricultural soils, both NO_3^-–N and NH_4^+–N increased with temperature; biochar had negligible effect on NH_4^+–N while significantly reducing NO_3^-–N at all temperatures (Table 2). This information together suggests that although warming enhanced nitrogen mineralization, subsequent nitrification and nitrate accumulation were constrained—either by limited nitrifier activity or by rapid NO_3^- adsorption/immobilization by biochar. Under such substrate limitation, microbial activity becomes less responsive to temperature fluctuations (Blagodatskaya et al. 2014; Zhang et al. 2020b), resulting in a lower Q_{10}.

The significantly lower Q_{10} in WH corresponded to its lowest NO_3^-–N and the smallest NO_3^--temperature slope (~ 0.01, Table S2). This may be related to wood biochar's larger pore size (49.6 nm) and highly aromatic surfaces (H:C = 0.26) (Table 1), which enhance nitrate immobilization through physical entrapment and π–cation interactions, further constraining substrate availability for denitrifiers (Cayuela et al. 2015; Tan et al. 2018). The pH increase at 10 ℃ under WH likely played a minor role relative to the strong NO_3^- constraint. qPCR data (available for WL/RL) showed no AOA enhancement and partial suppression of *nirS*/*nirK* genes at 30 ℃, suggesting that biochar did not amplify temperature-driven nitrification/denitrification.

4.6 Forest soil: tighter nitrification–denitrification coupling enhanced Q_{10}

In forest soils, WH significantly increased Q_{10} despite reducing cumulative N_2O emissions (Fig. 1) and NO_3^-–N content at higher temperatures (Table 2). This suggests that the mechanisms controlling Q_{10} in forest soils are not solely dependent on substrate limitation, but rather involve more complex microbial community responses (Zhang et al. 2023a).

Similar to agricultural soils, biochar had negligible effect on NH_4^+–N while significantly reducing NO_3^-–N at 20 ℃ (WH and WL) and 30 ℃ (all the biochar treatments). However, NH_4^+–N decreased while NO_3^-–N increased with temperature in forest soils. Moreover, biochar enhanced the magnitude of these responses with NH_4^+–N-temperature slopes becoming more negative (−0.36 to −0.47 vs −0.16 in CK), while WH and RH produced the smallest NO_3^-–N-tempertaure slopes (1.09 and 1.04 vs 1.46 in CK) (Table S2). These trends suggest that biochar accelerated NH_4^+ consumption while constraining net NO_3^-–N accumulation, implying tighter coupling between nitrification and nitrate-consuming processes (e.g., NO_3^- immobilization or denitrification). Such tighter coupling would increase the apparent temperature sensitivity of N_2O-producing pathways, leading to elevated Q_{10}.

Among biochar treatments, only WH showed a statistically significant increase in Q_{10}. Given the similar NO_3^--temperature response of RH but its non-significance, we interpret the WH effect cautiously. A plausible explanation lies in wood biochar's low ash content, higher aromaticity, and larger pore size, which promote short-term NO_3^- retention and create micro-scale redox gradients, thereby strengthening temperature-coupled nitrification–denitrification turnover.

Taken together, temperature determined the general magnitude of N_2O emissions, while biochar modified their temperature sensitivity by altering substrate availability and the degree of microbial coupling. The contrasting Q_{10} responses—reduction in agricultural soil but increase in forest soil under high-rate wood biochar—highlight that biochar-temperature interactions are context-dependent. In substrate-limited systems, biochar imposes constraints on microbial activity and dampens temperature sensitivity; in substrate-rich or microbial active systems, biochar may instead amplify thermal responsiveness through tighter coupling of N transformation pathways.

Future work should combine gross nitrification/denitrification assays, isotopic partitioning, more detailed analyses of microbial community composition and function (e.g., differentiation of *nosZ* clades I and II), together with comprehensive biochar characterization

(e.g., pore structure, surface functional groups, and nitrate-retention behavior), to elucidate the underlying mechanisms. Moreover, systematic investigations across multiple biochar types and soils are required to determine whether and how biochar modulates the temperature sensitivity of N_2O.

5 Conclusions

This study demonstrated how biochar affects the temperature sensitivity (Q_{10}) of soil N_2O emissions across two contrasting soil types. Effects of biochar on N_2O emissions were soil-dependent, i.e., variable in agricultural soils but consistently suppressive in forest soils. Notably, only high-rate wood biochar (WH) significantly altered Q_{10}, lowering it in agricultural soils while increasing it in forest soils, indicating that biochar effects on temperature sensitivity are both dose- and soil-specific.

The underlying physicochemical and microbial mechanisms differed between soils. In agricultural soils, biochar, particularly WH, decreased NO_3^-–N and intensified substrate limitation, leading to a lower Q_{10}. In forest soils, biochar enhanced the coupling between nitrification and denitrification, promoting stronger microbial responsiveness to temperature coupling. Wood biochar's low ash content, high aromaticity, and large pore size, likely promote short-term NO_3^- retention and create micro-scale redox gradients, thereby strengthening temperature-coupled nitrification–denitrification turnover, leading to higher Q_{10}.

PLS-PM modeling further revealed that temperature exerted stronger total effects on N_2O emissions than biochar, acting both directly and indirectly through shifts in substrate availability, pH, and microbial functional gene abundances. Biochar served as a secondary regulator, modulating but not overriding temperature-driven processes.

Overall, this study highlights that biochar's role in regulating the temperature sensitivity of N_2O emissions is context-dependent. Future work should integrate gross N transformation assays, isotopic tracing, and microbial functional analyses under long-term field conditions to better quantify how biochar-temperature interactions shape soil N_2O dynamics.

Supplementary Information

The online version contains supplementary material available at https://doi.org/10.1007/s42773-026-00591-2.

Supplementary Material 1.

Acknowledgements
We thank Zheng Su, Yongxin Shan, and Yue Liu for their help in soil collection.

Author contributions
Siyu Luo: Investigation, Methodology, Experiment, Data curation, Formal analysis, Writing-original draft. Zhibo Li: Investigation, Methodology, Data curation. Jing Hu: Methodology, Writing-review & editing. Xiaolin Liao: Conceptualization, Investigation, Methodology, Funding acquisition, Writing-review & editing.

Funding
This work was supported by the Natural Science Foundation of China (grant no. 42007090) and the Special Funds for Science and Technology Innovation on Carbon Peak Carbon Neutral of Jiangsu Province China (BK20220017).

Data availability
The datasets used or analyzed during the current study are available from the corresponding author upon reasonable request.

Declarations

Competing interests
The authors declare no conficts of interest.

Author details
[1]College of Ecology and Environment, Nanjing Forestry University, Nanjing 210037, Jiangsu, China. [2]Department of Civil, Environmental, and Construction Engineering, University of Central Florida, Orlando, FL 32816, USA.

Received: 8 June 2025 Revised: 6 February 2026 Accepted: 21 February 2026
Published online: 24 March 2026

References

Amato MT, Giménez D (2024) Predicting monthly near-surface soil temperature from air temperature and the leaf area index. Agric for Meteorol 345:109838. https://doi.org/10.1016/j.agrformet.2023.109838
Avrahami S, Conrad R (2003) Patterns of community change among ammonia oxidizers in meadow soils upon long-term incubation at different temperatures. Appl Environ Microbiol 69(10):6152–6164. https://doi.org/10.1128/AEM.69.10.6152-6164.2003
Blagodatskaya E, Zheng X, Blagodatsky S et al (2014) Oxygen and substrate availability interactively control the temperature sensitivity of CO_2 and N_2O emission from soil. Biol Fertil Soils 50:775–783. https://doi.org/10.1007/s00374-014-0899-6
Bond-Lamberty B, Thomson A (2010) Temperature-associated increases in the global soil respiration record. Nature 464(7288):579–582. https://doi.org/10.1038/nature08930
Butterbach-Bahl K, Baggs EM, Dannenmann M et al (2013) Nitrous oxide emissions from soils: how well do we understand the processes and their controls? Phil Trans r Soc B 368:20130122. https://doi.org/10.1098/rstb.2013.0122
Cayuela ML, van Zwieten L, Singh BP et al (2014) Biochar's role in mitigating soil nitrous oxide emissions: a review and meta-analysis. Agric Ecosyst Environ 191:5–16. https://doi.org/10.1016/j.agee.2013.10.009
Cayuela ML, Jeffery S, van Zwieten L (2015) The molar H: Corg ratio of biochar is a key factor in mitigating N_2O emissions from soil. Agric Ecosyst Environ 202:135–138. https://doi.org/10.1016/j.agee.2014.12.015
Clough T, Condron L, Kammann C et al (2013) A review of biochar and soil nitrogen dynamics. Agron J 3:275–293. https://doi.org/10.3390/agronomy3020275
Criscuoli I, Ventura M, Sperotto A et al (2019) Effect of woodchips biochar on sensitivity to temperature of soil greenhouse gases emissions. Forests 10(7):594. https://doi.org/10.3390/f10070594
Criscuoli I, Panzacchi P, Tognetti R et al (2024) Effects of woodchip biochar on temperature sensitivity of greenhouse gas emissions in amended soils within a mountain vineyard. Geoderma Reg 38:e00847. https://doi.org/10.1016/J.GEODRS.2024.E00847
Cui P, Fan F, Yin C et al (2016) Long-term organic and inorganic fertilization alters temperature sensitivity of potential N_2O emissions and associated

microbes. Soil Biol Biochem 93:131–141. https://doi.org/10.1016/j.soilbio.2015.11.005
Cui P, Chen Z, Fan F et al (2023) Soil texture is an easily overlooked factor affecting the temperature sensitivity of N_2O emissions. Sci Total Environ 862:160648. https://doi.org/10.1016/j.scitotenv.2022.160648
Dai Z, Yu M, Chen H et al (2020) Elevated temperature shifts soil N cycling from microbial immobilization to enhanced mineralization, nitrification and denitrification across global terrestrial ecosystems. Glob Chang Biol 26:5267–5276. https://doi.org/10.1111/gcb.15211
Davidson EA, Janssens IA (2006) Temperature sensitivity of soil carbon decomposition and feedbacks to climate change. Nature 440:165–173. https://doi.org/10.1038/nature04514
Deng B, Wang S, Xu X et al (2019) Effects of biochar and dicyandiamide combination on nitrous oxide emissions from *Camellia oleifera* field soil. Environ Sci Pollut Res Int 26(4):4070–4077. https://doi.org/10.1007/s11356-018-3900-3
Ding F, Sun W, Huang Y (2018) Net N_2O production from soil particle size fractions and its response to changing temperature. Sci Total Environ 650:97–104. https://doi.org/10.1016/j.scitotenv.2018.08.428
Hailegnaw NS, Mercl F, Pračke K et al (2019) Mutual relationships of biochar and soil pH, CEC, and exchangeable base cations in a model laboratory experiment. J Soils Sediments 19:2405–2416. https://doi.org/10.1007/s11368-019-02264-z
IPCC (2014) Climate change 2013: the physical science basis. State Dep Doc / FIND. https://doi.org/10.1017/CBO9781107415324
Joergensen RG, Mueller T (1996) The fumigation-extraction method to estimate soil microbial biomass: calibration of the k_{EN} value. Soil Biol Biochem 28(1):33–37. https://doi.org/10.1016/0038-0717(95)00101-8
Lehmann J, Rillig MC, Thies J et al (2011) Biochar effects on soil biota-a review. Soil Biol Biochem 43(9):1812–1836. https://doi.org/10.1016/j.soilbio.2011.04.022
Li Y, Zhang L, Fang S et al (2018) Variation of soil enzyme activity and microbial biomass in poplar plantations of different genotypes and stem spacings. J for Res 29:963–972. https://doi.org/10.1007/s11676-017-0524-2
Liao X, Chen Y, Ruan H et al (2021) Incapability of biochar to mitigate biogas slurry induced N_2O emissions: field investigations after 7 years of biochar application in a poplar plantation. Sci Total Environ 794:148572. https://doi.org/10.1016/J.SCITOTENV.2021.148572
Liao X, Chen Y, Hu J et al (2025) Effects of fresh and aged biochar on N_2O emission from a poplar plantation soil. Pedosphere 35(2):435–447. https://doi.org/10.1016/j.pedsph.2023.12.008
Liu Q, Zhang Y, Liu B et al (2018) How does biochar influence soil N cycle? A meta-analysis. Plant Soil 426:211–225. https://doi.org/10.1007/s11104-018-3619-4
Meyer N, Welp G, Amelung W (2018) The temperature sensitivity (Q_{10}) of soil respiration: controlling factors and spatial prediction at regional scale based on environmental soil classes. Glob Biogeochem Cycles 32(2):306–323. https://doi.org/10.1002/2017GB005644
Mukherjee A, Zimmerman AR (2013) Organic carbon and nutrient release from a range of laboratory-produced biochars and biochar–soil mixtures. Geoderma 193–194:122–130. https://doi.org/10.1016/j.geoderma.2012.10.002
Nguyen TTN, Xu C-Y, Tahmasbian I et al (2017) Effects of biochar on soil available inorganic nitrogen: a review and meta-analysis. Geoderma 288:79–96. https://doi.org/10.1016/j.geoderma.2016.11.004
Qi L, Pokharel P, Ni C et al (2020) Biochar changes thermal activation of greenhouse gas emissions in a rice–lettuce rotation microcosm experiment. J Clean Prod 247:119148. https://doi.org/10.1016/j.jclepro.2019.119148
Rittl TF, Oliveira DMS, Canisares LP et al (2021) High application rates of biochar to mitigate N_2O emissions from a N-fertilized tropical soil under warming conditions. Front Environ Sci. https://doi.org/10.3389/fenvs.2020.611873
Rogovska N, Laird D, Cruse R et al (2011) Impact of biochar on manure carbon stabilization and greenhouse gas emissions. Soil Sci Soc Am J 75(3):871–879. https://doi.org/10.2136/sssaj2010.0270
Schollenberger CJ, Simon RH (1945) Determination of exchange capacity and exchangeable bases in soil-Ammonium acetate method. Soil Sci 59(1):13–24
Song A, Liang Y, Zeng X et al (2018) Substrate-driven microbial response: a novel mechanism contributes significantly to temperature sensitivity of N_2O emissions in upland arable soil. Soil Biol Biochem 118:18–26. https://doi.org/10.1016/j.soilbio.2017.11.021
Sun L, Sang C, Wang C et al (2019) N_2O production in the organic and mineral horizons of soil had different responses to increasing temperature. J Soils Sediments 19:3499–3511. https://doi.org/10.1007/s11368-019-02316-4
Tan Z, Zou J, Zhang L et al (2018) Morphology, pore size distribution, and nutrient characteristics in biochars under different pyrolysis temperatures and atmospheres. J Mater Cycles Waste Manag 20:1036–1049. https://doi.org/10.1007/s10163-017-0666-5
Tian H, Xu R, Canadell JG et al (2020) A comprehensive quantification of global nitrous oxide sources and sinks. Nature 586(7828):248–256. https://doi.org/10.1038/s41586-020-2780-0
Tourna M, Freitag TE, Nicol GW (2008) Growth, activity and temperature responses of ammonia-oxidizing archaea and bacteria in soil microcosms. Environ Microbiol 10(5):1357–1364. https://doi.org/10.1111/j.1462-2920.2007.01563.x
Velthuis M, Veraart AJ (2022) Temperature sensitivity of freshwater denitrification and N_2O emission-a meta-analysis. Glob Biogeochem Cycles 36(6):e2022GB007339. https://doi.org/10.1029/2022GB007339
Wu J, Joergensen RG, Pommerening B et al (1990) Measurement of soil microbial biomass C by fumigation-extraction-an automated procedure. Soil Biol Biochem 22:1167–1169. https://doi.org/10.1016/0038-0717(90)90046-3
Wu L, Xiao Q, Wang J et al (2022) Liming decreases the emission and temperature sensitivity of N_2O following labile carbon addition. Geoderma 425:116032. https://doi.org/10.1016/J.GEODERMA.2022.116032
Xia L, Cao L, Yang Y et al (2023) Integrated biochar solutions can achieve carbon-neutral staple crop production. Nat Food 4:236–246. https://doi.org/10.1038/s43016-023-00694-0
Xing X, Tang Y, Xu H et al (2021) Warming shapes nirS-and nosZ-type denitrifier communities. Appl Environ Microbiol 87:e02965-e3020. https://doi.org/10.1128/AEM.02965-20
Yang Y, Li T, Pokharel P et al (2022) Global effects on soil respiration and its temperature sensitivity depend on nitrogen addition rate. Soil Biol Biochem 174:108814. https://doi.org/10.1016/j.soilbio.2022.108814
Yao J, Wang X, Hong M et al (2025) Response of soil pH to biochar application in farmland across China: a meta-analysis. PeerJ 13:e19400. https://doi.org/10.7717/peerj.19400
Yu L, Li M, Kang X et al (2025) Climate warming plays an important role in dissolved organic carbon loss in deep soil layers across China. CATENA 259:109404
Zhang Y, Wang J, Dai S et al (2019) Temperature effects on N_2O production pathways in temperate forest soils. Sci Total Environ 691:1127–1136. https://doi.org/10.1016/j.scitotenv.2019.07.208
Zhang H, Yao X, Zeng W et al (2020a) Depth dependence of temperature sensitivity of soil carbon dioxide, nitrous oxide and methane emissions. Soil Biol Biochem 149:107956. https://doi.org/10.1016/j.soilbio.2020.107956
Zhang Y, Zhang N, Yin J et al (2020b) Combination of warming and N inputs increases the temperature sensitivity of soil N_2O emission in a Tibetan alpine meadow. Sci Total Environ 704:135450. https://doi.org/10.1016/j.scitotenv.2019.135450
Zhang C, Miao Y, Malghani S et al (2023a) Biochar combined with different nitrogen fertilization rates increased crop yield and greenhouse gas emissions in a rapeseed-soybean rotation system. J Environ Manage 345:118915. https://doi.org/10.1016/j.jenvman.2023.118915
Zhang X, Jiao Y, Wang B et al (2023b) Biochar amendments and climate warming affected nitrification associated N_2O and NO production in a vegetable field. J Environ Manage 330:117178. https://doi.org/10.1016/j.jenvman.2022.117178
Zhou J, Delgado-Baquerizo M, Vancov T et al (2025) Biochar mitigates nitrogen deposition-induced enhancement of soil N_2O emissions in a subtropical forest. Biol Fertil Soils. https://doi.org/10.1007/s00374-025-01899-0